Reprinted from
PROGRESS IN HEAT & MASS TRANSFER VOLUME 7
Edited by
O.E. DWYER
PERGAMON PRESS–OXFORD & NEW YORK–1973.

BOILING OF MERCURY IN A VERTICAL TUBE UNDER FORCED-FLOW CONDITIONS

H. SCHMÜCKER and U. GRIGULL
Institut A für Thermodynamik, TU München

Abstract. The hydrodynamic and boiling behaviour of pure mercury in a vertical tube at low exit pressures was investigated. Stable and unstable operating modes were found. At the tube exit, maximum mass flow rate was always established. Heat transfer rates in the non-wetting system are in the range of the values obtained for mercury vapour cooling by forced convection. Visualization of the boiling zone and mercury two-phase flow was obtained by X-ray photography. Any similarity to well-known flow patterns was not found.

NOMENCLATURE

c_p	specific heat
D	tube inner diameter
E	energy
g	gravity acceleration
K_s	mixture compressibility
L	tube length
$\dot{m}/F$	mass flow rate, $\dot{m}$ mass flow
P	pressure
q	heat flux
r	latent heat of vaporization
S	slip ratio
U	$= D\pi$, $F = D^2\pi/4$
v'	specific volume of liquid
v''	specific volume of vapour
w'	velocity of liquid
w''	velocity of vapor
x	quality
$\bar{x}$	quality in the boiling zone
z	height
$\bar{z}$	length of boiling zone

Subscripts

A	exit
E	entrance
S	saturation

α	void fraction
ϑ	temperature
ρ	density
χ	isentropic exponent

INTRODUCTION

With the development of fast-breeder reactors, the scientific investigation of liquid-metal boiling behaviour became one of the most important contributions to nuclear safety. The coolant of nearly all research programs was and still is sodium and potassium or their eutectic mixture. Less attention has been paid to pure mercury experiments, at least under the condition of forced convection. An early investigation in 1940 by Styrikovich *et al.* [1] found the boiling coefficient for mercury to be considerably lower than that for single phase forced-convection. With the development of the SNAP Reactor [2–5], research activity increased, and certain aspects of boiling phenomena were examined. C. R. Smith *et al.* [6] studied slip velocity in two-phase mercury flow and found a considerable deviation in values compared to non-metallic fluids.

An extensive study on mercury boiling in a tube was performed by Gelman and Kopp [7]. In their equipment, they used a tube made of mild steel and obtained heat-transfer rates indicating nucleate boiling after heating up the tube to 800°C for a long period.

In the present study, the hydrodynamic and thermal behaviour of boiling pure mercury at low pressures in a vertical tube was investigated. The varied parameters were the mass flow rate, the heat load, and inlet and outlet temperatures.

THE EXPERIMENTAL APPARATUS

Basically, the experimental set-up was a closed-loop configuration for handling the mercury and its vapour. The loop was kept under a high vacuum of 10^{-3} torr, the vapour pressure of mercury at 25°C. Special care was taken to maintain the purity of the used fluid for a long test period. No protecting gas was applied, in order to exclude its unknown influence on boiling characteristics. Corrosion attack of mercury on steel, even at high temperatures, was avoided by carefully selecting the most corrosion-resistant construction material for all parts in contact with mercury. The simplified test equipment is shown in Fig. 1.

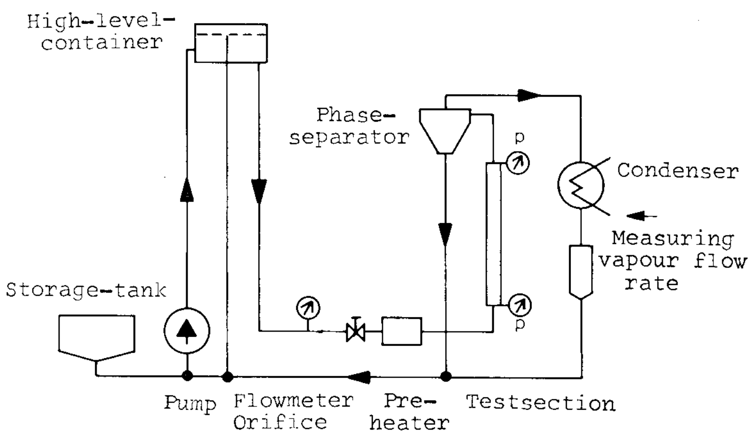

FIG. 1. The basic layout of the experimental set-up.

A spiral induction pump supplied mercury to a high-level container to ensure constant inlet pressure at the test section. From the bottom tube of this container, mercury flowed down to both an orifice and an electromagnetic flowmeter to measure mass flow rates. After passing a throttling valve for mass flow rate limitation, the mercury entered the preheater section, where the fluid could be heated up to 300°C at mass flow rates up to 650 kg/m^2 s. In the test section, the mercury was partly evaporated, and the two-phase mixture entered the phase separator at the top of the test section. The fluid portion was fed back to the pump inlet, while the vapour was condensed in a concentric tube, cooled by Dowtherm. After flowing through a flowmeter, that portion of mercury was also fed back to the pump.

The test section was a stainless-steel tube of ferritic quality with an i.d. of 14.17 mm and a total length of 800 mm. The outer surface was insulated, and a heating tape was wound around the tube, so that a constant heat flux up to 10 W/cm^2 could be applied over a length of 700 mm by d.c. heating. Twenty-one thermocouples were equally spaced along the tube and were attached to the tube wall. Four shielded thermocouples were mounted in the centre of the tube, each ending at a different height opposite a wall thermocouple. Inlet and outlet pressures were measured by pressure transducers of high sensibility and good frequency response (> 100 Hz). Also measured are average inlet and outlet temperatures.

All temperatures, mass flowrates, and pressures were recorded on a data acquisition system having a repetition time of 7 sec per channel. Inlet pressure and mass flow rate were recorded also on a two-channel analog plotter.

EXPERIMENTAL PHENOMENA

In the course of the experimental tests, three different types of boiling phenomena were observed. Beginning with low inlet temperatures and heat loads, the mercury column in the tube started to boil at the upper end, and the boiling zone travelled down to an upstream

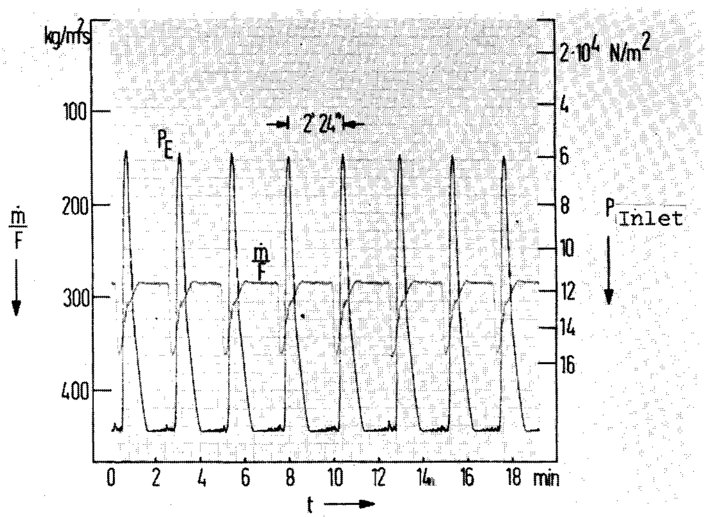

FIG. 2. The pulsating boiling mode. Data recording from the two-channel analog plotter. The high peaks demonstrate the inlet pressure excursions P_E when the boiling zone travels upstream. Also shown are the variations of the mass flow rate $\dot{m}/F$.

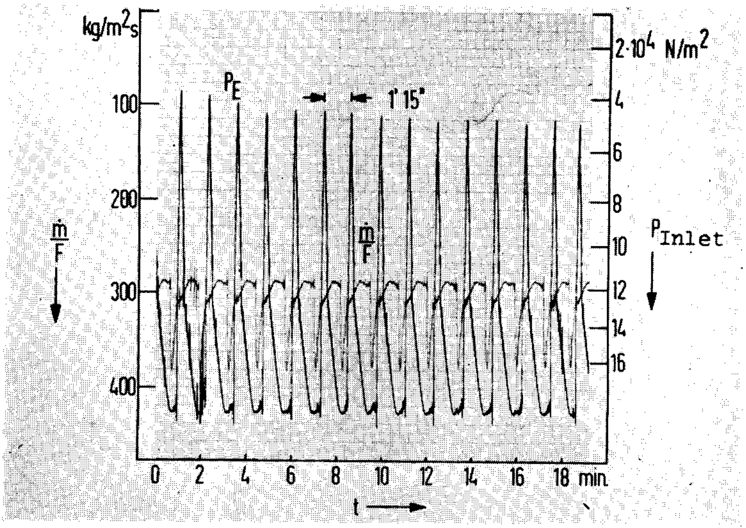

FIG. 3. The pulsation boiling mode performing with higher frequency.

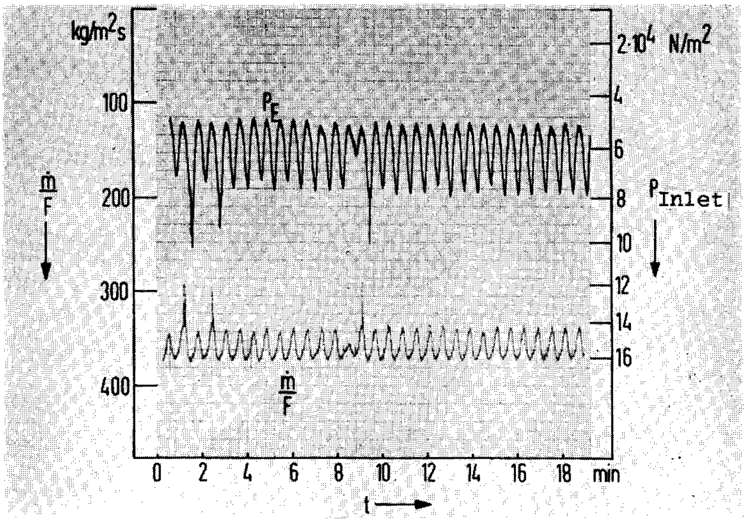

FIG. 4. Nearly stable boiling operation with small pressure fluctuations.

position, where it remained for a while. Then vapour production decreased and the tube was filled again with liquid mercury. This behaviour was repeated periodically, with repetition times of 1 to 3 min. Figure 2 shows a typical graph of both the inlet-pressure excursions and the related variation in mass flow rate. In Figure 3 the same event is shown occurring with higher frequency under modified parameters. When the exit temperature was increased, the boiling zone began to move downwards, but stayed at a certain height, and boiling continued either with small pressure fluctuations as shown in Fig. 4, or under completely stable conditions. By increasing temperatures further, the boiling zone did not stabilize in the tube but travelled upstream out of the test section. When that happened, shut-down was necessary, to protect the preheater section from damage.

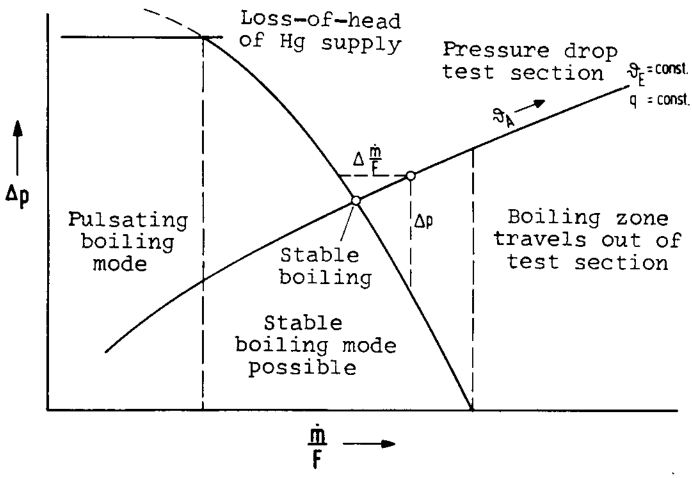

FIG. 5. The loss-of-head line of the mercury supply and the pressure drop curve of the boiling tube for constant heat load q and inlet temperature ϑ_E.

This behaviour is explained by Fig. 5. It shows the loss-of-head for the high-level container with the orifice and throttling valve further downstream versus the mass flow rate. The line going from the lower left to upper right represents a characteristic curve of the test section for the condition of constant inlet temperature and heat load. Any point on the curve represents a definite exit temperature. The development of this curve will be given later on. The crosspoint of both curves gives the stable operating point with all the related parameters. For a higher exit temperature, the tube is able to transport a higher mass flow rate at a higher pressure drop. As this operating point has no corresponding point on the loss-of-head line, the pressure drop will vary by Δp, and also the mass flow rate by $\Delta \dot{m}/F$. If the operating point comes beyond the horizontal part of the loss-of-head line, only periodic boiling occurs, as shown in Figs. 2 and 3. For operating conditions beyond the maximum mass flow rate of the loss-of-head line, the boiling zone travels upstream out of the test section.

TUBE EXIT CONDITIONS

This boiling behaviour indicates a strong dependence on exit parameters. Estimated vapour velocities at the tube outlet were in the order of sonic speed at outlet temperatures. So the assumption seems to be justified that maximum mass flow rate (chocked flow) existed at the exit of the test tube. Several runs were made with the system, measuring only mass flow rate, exit temperature, and quality. The total mass flow rates were in the range of 200–450 kg/m^2 s, exit temperatures varied from 180°C to 210°C, while the quality range extended from 4% to 8%.

To correlate these data, Moody's model for two-phase critical flow [8] was applied in a simplified form. For a separate two-phase flow-mixture, Moody provides the following relationship:

$$(\dot{m}/F)^2 = \frac{1}{K_s}\left[\frac{\alpha^3}{x^2}\cdot\frac{1}{v''} + \frac{(1-\alpha)^3}{(1-x)^2}\cdot\frac{1}{v'}\right] \tag{1}$$

with the mixture adiabatic compressibility

$$K_s = -\left[\frac{\alpha}{v''}\left(\frac{\partial v''}{\partial p}\right)_s + \frac{1-\alpha}{v'}\left(\frac{\partial v'}{\partial p}\right)_s\right]. \tag{2}$$

For mercury at low pressures, a number of simplifications can be applied. As the compressibility of liquid mercury is very small, and mercury vapour performs like an ideal gas, the mixture compressibility reduces to

$$K_s = \frac{1}{\chi P}. \tag{3}$$

The relationship between quality, void fraction, and slip,

$$S = \frac{x}{1-x}\,\frac{1-\alpha}{\alpha}\,\frac{v''}{v'}, \tag{4}$$

shows that even for small values of the quality x at slip ratios S in the order of 100, void fraction α approaches 1 due to the specific volume ratio of

$$\frac{v''}{v'} = 10^5$$

at temperatures around 200°C.

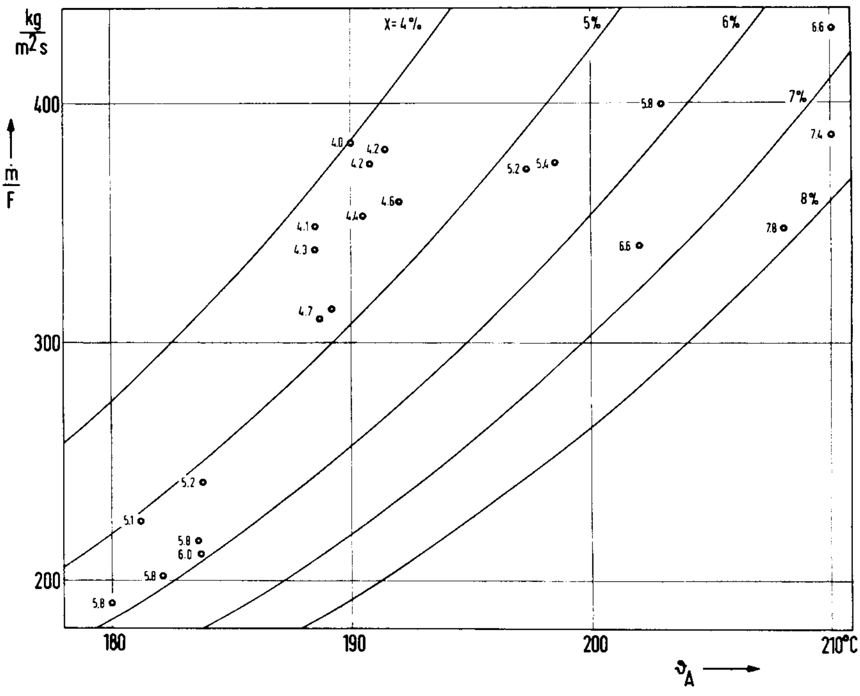

FIG. 6. The critical mass flow rate versus exit temperature.

In respect of these simplifications, eqn. (1) reduces to

$$(\dot{m}/F)^2 = \chi P \frac{1}{x^2} \frac{1}{v''}. \tag{5}$$

In Fig. 6 the critical mass flow rate, $\dot{m}/F$, is shown versus exit temperature. The parameter is the quality x. The points indicate the test results, with the measured qualities shown beside them. Figure 7 indicates the agreement of prediction by eqn. (5) with the test results. The deviation is less than $\pm 10\%$. Considering the strong dependence of the critical mass flow rate on the measured exit temperature, e.g. a change of temperature by 1% results in a 7% change of the mass flow rate, the accuracy of the test results seems to be reasonable.

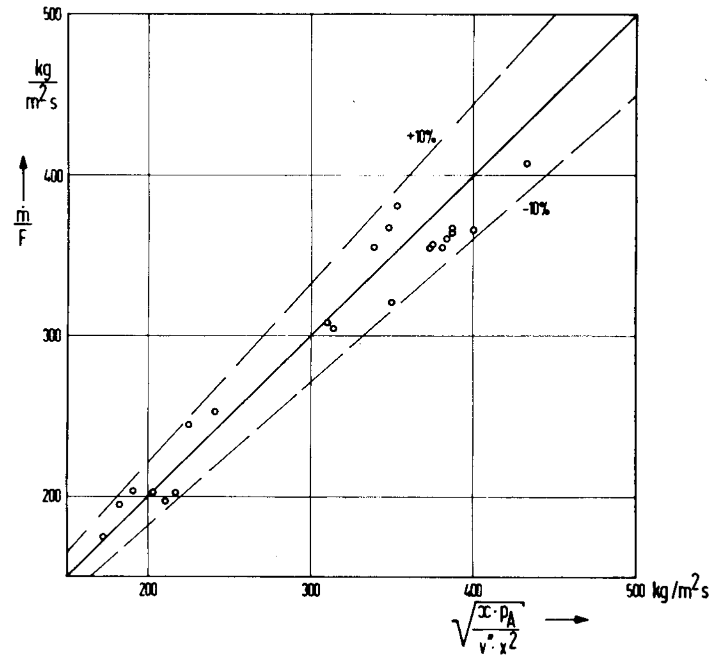

FIG. 7. Comparison between measurements and prediction, eqn. (5), of the critical mass flow rate.

THE PRESSURE-DROP MODEL

The main pressure drop in the test section is due to the hydrostatic head of the liquid mercury column. In the two-phase region, pressure drop will be caused mainly by acceleration and friction. So the overall pressure drop is

$$\Delta P = \rho' g z + \Delta P_{\text{acc}} + \Delta P_{\text{f}}. \tag{6}$$

where z is the height of the liquid column from inlet to the boiling zone. Having a non-wetting system, the liquid mercury will rarely be in contact with the tube wall in the two-phase region and therefore the frictional pressure loss will be caused by the vapour streaming along the wall. Presuming all mercury would be evaporated and would stream with the corresponding velocity, it will cause a frictional pressure drop not exceeding 200 N/m², for the maximum mass flow rate used in the tests. As this value is lower by two orders of magnitude compared to the aforementioned pressure drops, friction will be neglected.

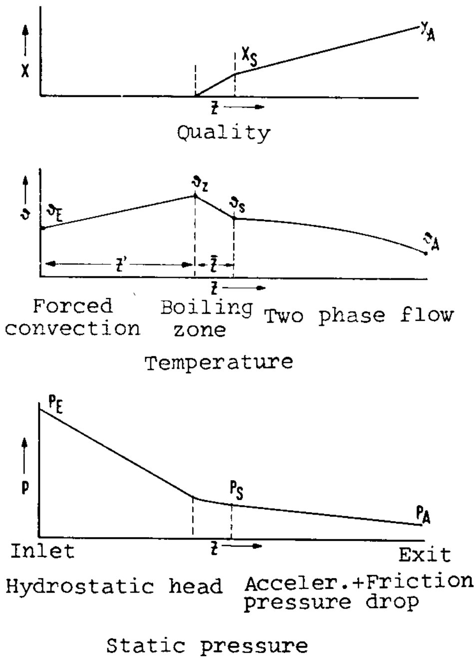

FIG. 8. Assumed quality, temperature, and pressure distribution along the tube.

For this model the assumed pressure, temperature and quality distributions along the tube are shown in Fig. 8. From the inlet to the beginning of the boiling zone, pressure decreases linearly with height. The temperature will first follow the law of forced-convection heat transfer. In the boiling zone a sharp temperature drop will occur due to rapid vapour production. The quality x increases to about 25% of its final value. In the two-phase region, pressure drops steadily and so does the fluid temperature, when assuming thermodynamic equilibrium between the two phases. Due to free-stream evaporation, the quality x increases. Using the energy equation, z can be given by

$$z = (\vartheta_Z - \vartheta_E)\,\frac{(\dot{m}/F)\,c_P F}{qU}. \tag{7}$$

The energy for vapour production in the boiling zone is delivered from the liquid mercury:

$$\vartheta_Z - \vartheta_S = \frac{\bar{x} r}{c_P}. \tag{8}$$

The energy for the vapour production further downstream results from the applied heat load to the tube wall, as well as from the temperature loss of the mercury remaining in liquid phase.

$$\dot{m}(x - \bar{x})r = \dot{m}(1 - \bar{x})\, c_P(\vartheta_S - \vartheta_A) + qU(L - z - \bar{z}). \tag{9}$$

Combining eqns. (7), (8) and (9), and having in mind eqn. (5), the height z is given by

$$z = \left[(\vartheta_S - \vartheta_E) - \frac{r}{c_P}\left(\frac{\vartheta_S - \vartheta_E}{\vartheta_S - \vartheta_A} - 1\right) - x\,\frac{r^2}{c_P^2}\frac{1}{\vartheta_S - \vartheta_A}\right]\frac{\dot{m}}{F}\frac{Dc_p}{4q} - \frac{L - \bar{z}}{c_P/r(\vartheta_S - \vartheta_A)}. \tag{10}$$

The pressure drop in the two-phase region can be calculated by the momentum equation for separated flow, neglecting the velocity of the liquid fluid at the boiling zone.

$$P_S - P_A = \frac{\dot{m}}{F}[(1 - x)\, w' + xw'']. \tag{11}$$

Introducing eqns. (4) and (5), the pressure ratio becomes

$$P_S/P_A = 1 + \chi\left(\frac{1 - x}{x}\frac{1}{S} + 1\right). \tag{12}$$

The quality x can be evaluated from an over-all energy balance for the tube

$$E_{\text{input}} = E_{\text{output}}, \tag{13}$$

and the boiling temperature is related to P_s by the vapour–pressure–temperature relationship.

So, the overall pressure drop is given by

$$\Delta p = \rho' g z + P_S - P_A. \tag{14}$$

When the measured pressure drop is compared with this simple model, the mean deviation does not exceed $\pm 15\%$. Figure 9 shows the pressure drop versus mass flow rate for different heat loads and inlet temperatures. The crossing lines represent loss-of-head at two different throttle-valve settings.

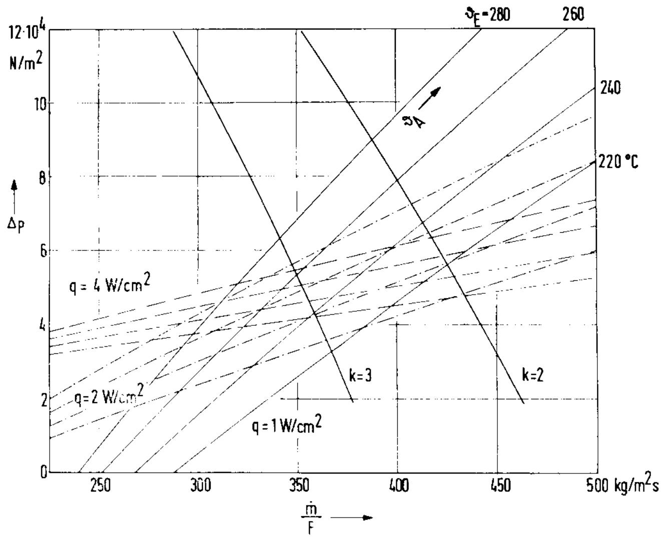

FIG. 9. Pressure drop versus mass flow rate for various parameters.

HEAT TRANSFER IN THE TWO-PHASE REGION

When stable boiling conditions were achieved, temperature measurements were made along the tube wall and at certain points along the tube axis. Even at small heat loads, the wall temperature at the outlet exceeded 600°C.

As thermocouples were soldered to the wall, the maximum safe temperature was limited to 630°C. The temperature difference between wall and fluid reached 400°C, indicating vapour cooling at least at the end of the test section.

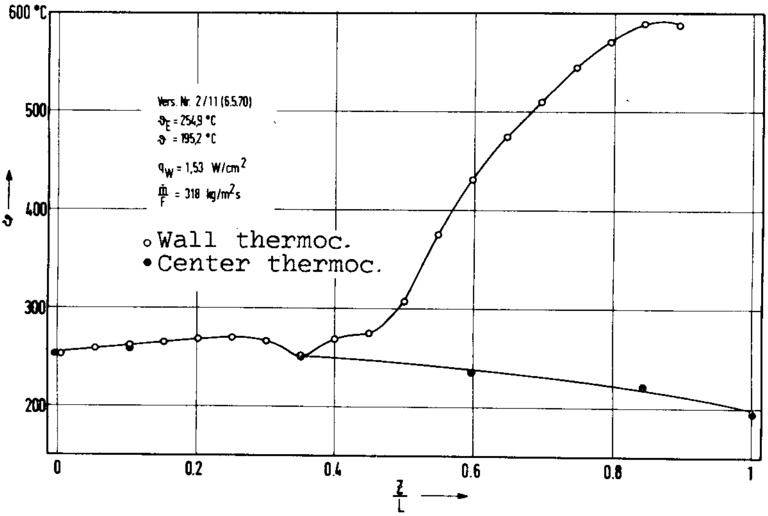

FIG. 10. Typical temperature distribution along the tube wall and the tube axis.

A typical temperature distribution is given in Fig. 10. Black points are temperatures in the centre, while open points are wall temperatures. A slow and steady rise indicates the forced-convection of liquid mercury in the lower part of the tube. In the boiling zone a temperature drop occurs due to vapour production. Then the temperature of the two-phase flow slowly decreases, while wall temperature rises to nearly 600°C. The heat load applied in this run was 1.53 W/cm², and the mass flow rate was 318 kg/m² s.

Several runs were performed with different parameters and an example of the results is shown in Fig. 11.

The horizontal axis represents a dimensionless height $(z - z_P)/L$, where z_P is the height of the liquid mercury column evaluated from pressure-drop measurements. L is the total length of the test section. On the vertical axis are plotted heat-transfer ratios α_z/α_A where α_A is the heat transfer rate at the exit of the tube. These heat transfer rates were compared to Nusselt numbers calculated under the assumption that mercury vapour alone completely fills the cross-section. For gases with Prandtl numbers between 0.1 and 1 and turbulent flow, Kays [9] suggests the equation

$$Nu = 0.022\, Pr^{0.6}\, Re^{0.8}. \tag{15}$$

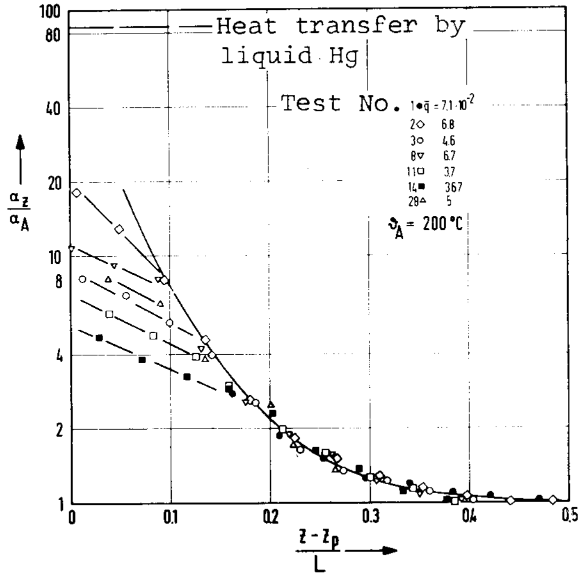

FIG. 11. Reduced heat transfer rates along the tube from the boiling zone to the exit.

The measured Nusselt numbers at the end of the test section are higher. For all tests, the ratio of experimental Nusselt number Nu_A to Nu by eqn. (15) was

$$\frac{Nu_A}{Nu} = 4.83 \pm 0.35. \tag{16}$$

This factor represents the higher heat-transfer rate due to undeveloped turbulent flow, momentum exchange between the two phases, and void fraction less than 1.

In Fig. 9 are also shown the heat-transfer rates in the boiling zone. Here, the influence of the mass flow rate is evident.

TWO-PHASE FLOW VISUALIZATION BY X-RAY PHOTOGRAPHY

The interpretation of the heat-transfer measurements, in view of the two-phase flow pattern, may lead to the assumption that a reversed annular flow exists. Stability considerations suggest, however, that such a flow system is rather improbable. In order to get more information about the boiling regime and the two-phase flow behaviour, it was necessary to observe the processes in the tube by X-ray technique. The existence of critical mass flow rate at the exit of the test section indicates extremely high velocities of vapour and liquid mercury. Therefore, a pulsed X-ray beam source was used that gave exposure times of 30 nanosec and repetition frequencies of 10 shots per second. A drum-camera was constructed and equipped with X-ray amplification foil. Figure 12 shows the set-up. The X-ray tube and the drum camera could be moved in the axial direction, so that any cross-section could be photographed. At least forty pictures of each section, 130 mm long, were taken, beginning from the upper end and moving downward to the boiling zone. Figure 13 is a typical picture of the boiling zone. Because of non-wetting, no nucleate boiling occurs, but the vapour cushion next to the wall grows very rapidly and occupies a considerable part

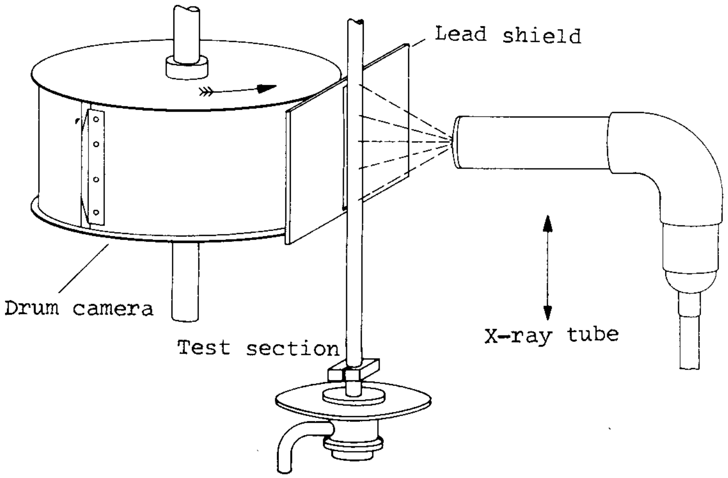

FIG. 12. Set-up for X-ray photography.

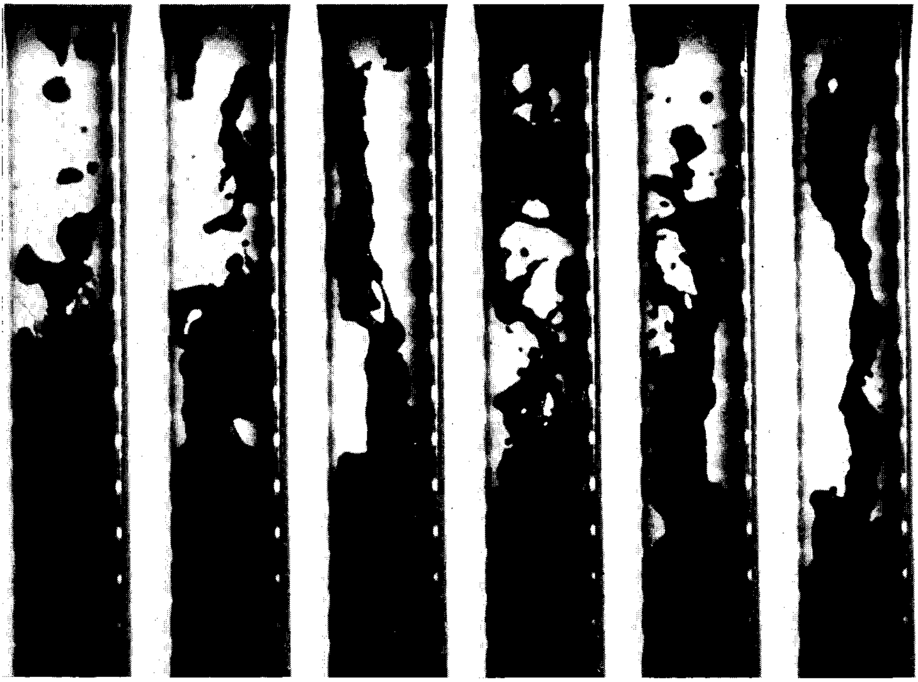

FIG. 13. Boiling zone.

of the cross-section, even at the beginning of boiling. Sometimes, reversed annular flow exists for a very few moments. Due to the high vapour velocities, the life of a liquid column is limited. Further downstream, the liquid phase scatters more and more (Fig. 14) as the vapour-accelerating forces increase. Though the quality is in the region of only 5%, large sections of the tube are filled with vapour already. Particles entering the lower edge of the

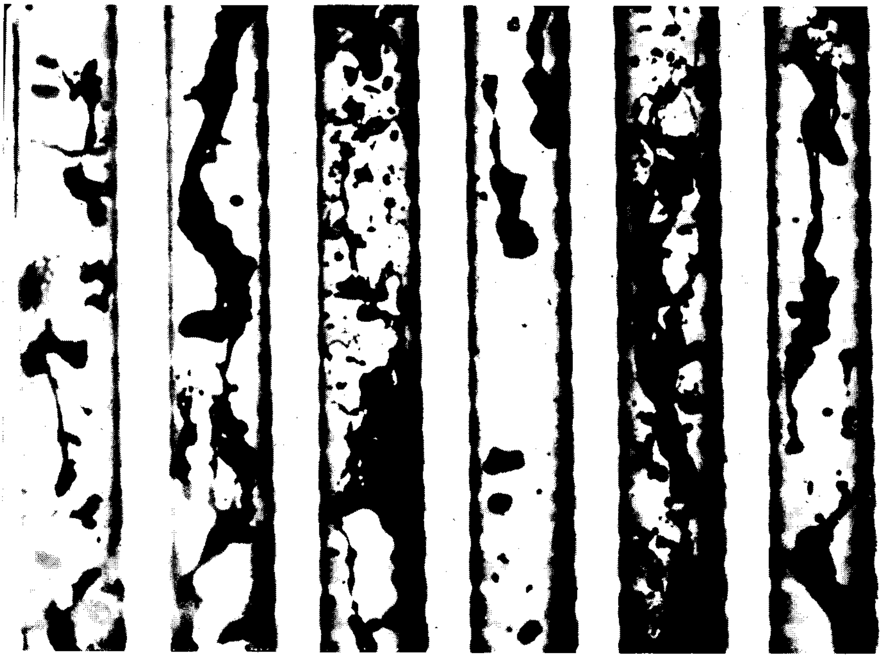

FIG. 14. Two-phase region.

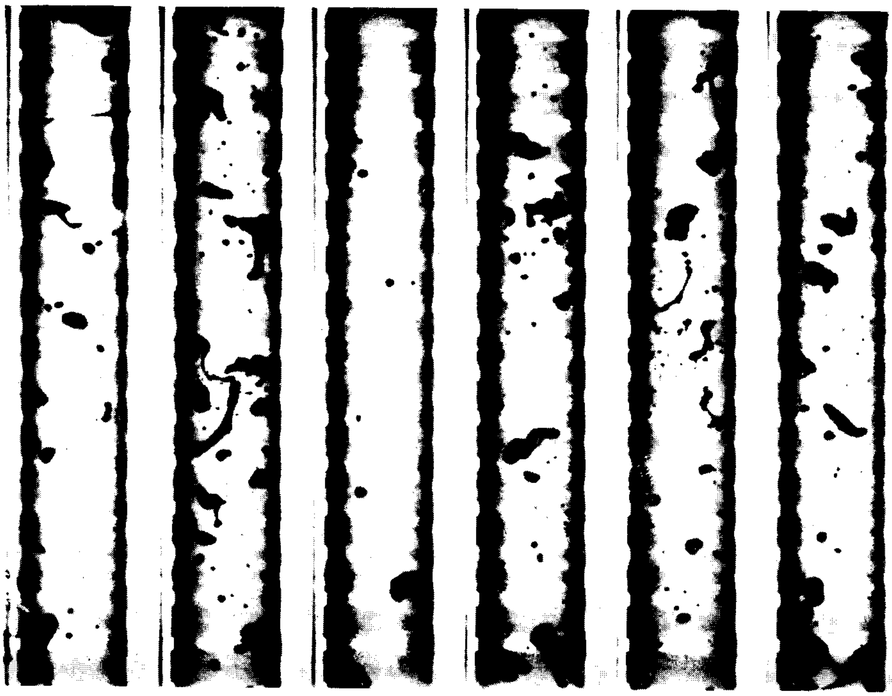

FIG. 15. Tube exit section.

picture frame cannot be identified on the following picture although the delay time is one-tenth of a second. This indicates a particle speed of more than 1.3 m/s just downstream from the boiling zone. At the exit cross-section shown in Fig. 15, the liquid phase is completely dispersed into small droplets, and the void fraction is close to one. The velocity, limited by the critical mass flow rate, is of the order of the sonic velocity (~ 150 m/s). The slip ratio certainly does not > 100.

To determine particle speed from such pictures, and to be able to give exact information on slip ratios, the frame frequency should be an order of magnitude higher. Such an installation was not available at the time the experiments were done.

CONCLUSIONS

The boiling behaviour of pure mercury under reduced pressure conditions has been studied. It was found that critical mass flow rate was always established at the exit of the tube. A simple pressure-drop model was developed that represented the measured values within $\pm 15\%$. Heat transfer rates at the exit were higher than those evaluated on the basis of 100% vapour flow.

X-ray pictures of the boiling zone showed rapidly growing vapour cushions at the tube wall. In the two-phase region, the liquid phase was completely scattered, although the quality was very low. In this non-wetting system, the observed flow pattern was different from the usually observed two-phase flow characteristics.

REFERENCES

1. Styrikovich, M. A. and Semenovker, I. E., *J. Techn. Phys.* (*U.S.S.R*), **10**, no. 16, 1331 (1940).
2. An evaluation of mercury cooled breeder reactors, Adv. Techn. Lab. 31. Okt. 1959, ATL-A-102, TiD 4500.
3. Iicha, J. and Keenan, J. J., Mercury boiler development. MND-P-2309, June 1960.
4. Kiraly, R. J. and Koestel, A., SNAP II power conversion system, NAA-SR-6301 (1961).
5. *The SNAP II Power Conversion System*, Topical Report No. 1.7, Mercury Boiling Research, NAA-SR-6309.
6. Smith, C. R. *et al.*, Measurement of slip velocity in two-phase mercury flows, *A.I.Ch.E. J.* **10** (4), 568 (1964).
7. Gelman, L. I. and Kopp, I. Z., Heat transfer in nucleate boiling of mercury at thermal loads up to $2 \cdot 10^6$ W/m^2. *High Temperature* **6** (3), 532 (1968).
8. Moody, F. J., A pressure pulse model for two-phase critical flow and sonic velocity. *J. Heat Transfer*, **91**, 371 (1969).
9. Kays, W. M., *Convective Heat and Mass Transfer*, McGraw-Hill Co., 1966.